A Study on the Removal Characteristics of Nickel Ion from Wastewater by Low-Cost Nano Adsorbent

R Sivakumar, S Arivoli[*] ,V Marimuthu

[*]PG and Research Department of Chemistry, Thiru Vi Ka Government Arts College, Thiruvarur, Tamilnadu, India.

Abstract—The work aims at adsorption studies of nickel from aqueous solution onto activated nano carbon prepared from Syringodium Isoetifolium Leaves, by acid treatment was tested for its efficiency in removing nickel ion. The process parameters studied include agitation time, initial nickel ion concentration, adsorbent dose, pH and temperature. The adsorption followed second order reaction equation and the rate is mainly controlled by intra-particle diffusion. The equilibrium adsorption data were correlated with Langmuir, Freundlich, Temkin, Dubinin-Radushkevich, Hurkins-Jura, Halsay, Redlich-Peterson, Jovanovich and BET isotherm models. The adsorption capacity (Q_m) obtained from the Langmuir isotherm plot at an initial pH of 6.5 and at 30, 40, 50, 60 ± 0.5 ^{0}C. The influence of pH on nickel ions removal was significant and the adsorption was increased with increase in temperature. A portion of the nickel ion was recovered from the spent ASI-NC using 0.1M HCl.

Keywords—Activated Syringodium Isoetifolium Leaves Nano Carbon (ASI-NC), Adsorption isotherm, Equilibrium, Intra-particle diffusion. Nickel ion, Thermodynamic parameters.

I.   INTRODUCTION

Heavy metal pollution of water and water bodies is a serious environmental problem that affects the quality of water. The consequences are decreasing water supply, increase in cost of purification, eutrophication of water bodies and decrease in aquatic production [1]. In order to tackle the menace poise by heavy metal pollution of water, several options have been adopted. These include oxidation and reduction, chemical precipitation, filtration, electrochemical treatment, ion exchange, membrane separation, reverse osmosis, adsorption, evaporation and electrolysis [2]. However, adsorption has been proven to be one of the best options available for the removal of heavy metals from aqueous solution [3]. In view of the above, several researches have been conducted using various materials as adsorbents [4]. However, some of these adsorbents also contain other toxicants; some are

expensive and are characterized with limited surface area for adsorption.

A search of literature revealed that fruit stone has been used for adsorption of some heavy metals from aqueous solution but literature is scanty on the use of activated carbon produced from fruit stone for the adsorption of nickel ions from aqueous solution. Therefore, the objective of the present study is to investigate the possibility of using ASI-NC.

II.   MATERIALS AND METHODS

2.1. Adsorbent

The *Syringodium Isoetifolium* Leaves collected from East Coastal area of Nagapattinam district was Carbonized with concentrated Sulphuric Acid and washed with water and activated around 1000°C in a muffle furnace for 5 hrs the it was taken out, ground well to fine powder and stored in a vacuum desiccators.

Syringodium Isoetifolium

2.2. Chemicals

All chemicals used of high purity commercially available Analar grade. 1000 mg/L of stock solution of nickel was prepared by dissolving accurately weighed 4.4786 gram of nickel sulphate in 1000 ml distilled water. All experimental solutions were prepared by diluting the stock solution to the required concentration. The pH of each experimental solution was adjusted to the required initial pH value using dilute HCl (or) NaOH before mixing the adsorbent. The concentration of residual nickel ion was determined with atomic absorption spectrophotometer (Perkin Elemer 2380).

2.3. Batch experiments

The effect of various parameters on the removal of nickel ion onto ASI-NC was studied batch adsorption experiments were conducted at (30-60°C). For each experimental run, 50 ml of nickel solution of known initial concentration and pH were taken in a 250 ml plugged conical flask. A 25 mg adsorbent dose is added to the solution and mixture was shaken at constant agitation speed (150 rpm) sample were withdrawn at appropriate time intervals (10-60 min) and the adsorbent was separated by filtration. The residual solutions were analyzed to determine the nickel ion concentration.

The effect of dosage of adsorbent on the removal of nickel ion was measured by contacting 50 ml of 50 mg/L of nickel ion solution with 25 mg of ASI-NC till equilibrium was attained. Adsorption equilibrium isotherm is studied using 25 mg of ASI-NC dosage per 50 ml of nickel ion solution. The initial concentration were ranged from (10 to 50 mg/L) in all sets of experiments. The plugged conical flask was shaken at a speed of 150 rpm for 60 minutes. Then the solution was separated from the mixture and analyzed for nickel ion concentration. The adsorption capacity was calculated by using a mass equilibrium equation as follows:

$$q_e = (C_0 - C_e) V/M \quad \text{.............................} \quad (1)$$

Where, C_0 and C_e being the initial nickel concentration (mg/L) and equilibrium concentration, respectively V is the experimental volume of nickel ion solution expressed in liters [L] and M is the adsorbent mass expressed in grams [g]. The nickel ion ions percentage can be calculated as follows:

$$\%R = (C_0 - C_t) \times 100/C_0 \quad \text{.....................} \quad (2)$$

The effect of pH on the rate of adsorption was investigated using nickel concentration of 20 mg/L constant ASI-NC dosage. The pH values were adjusted with dilute HCl and NaOH solution. The adsorbent-adsorbate mixture was shaken at room temperature using agitation speed (150 rpm) for 60 minutes. Then the concentration of nickel in solution was determined.

III. RESULTS AND DISCUSSION

3.1 Effect of agitation time and initial Nickel ion concentration

The kinetics of adsorption of nickel ion by ASI-NC is shown in Fig. 1 with smooth and single plots indicating monolayer adsorption of nickel ions on the ASI-NC. The removal of nickel ions increased with the lapse time and attains equilibrium in 60 min for 50 mg/ L. With increase in nickel ions concentration from 10 to 50 mg/L, the amount of nickel ions adsorbed increased while the percent removal decreased, indicating that the nickel ions removal by adsorption on ASI-NC concentration dependent.

3.2 Effect of ASI-NC mass

The amount of nickel ion adsorption increased with the increase in ASI-NC dose and reached a maximum value after a particular dose shown in Fig. 2 and taken an initial nickel ions concentration of 20 mg/L, complete nickel ions removal was obtained at a maximum ASI-NC dose of 125 mg. The increase in the adsorption of nickel ions with ASI-NC dose was due to the introduction of more binding sites for adsorption and the availability more surface area.

3.3 Effect of pH

The experience carried out at different pH show that there was a change in the percentage removal of nickel ions over the entire pH range shown in Fig. 3. This indicates the strong force of interaction between the nickel ions and ASI-NC that either H^+ or OH^- ions could influence the adsorption capacity. In other words, the adsorption of nickel ions on ASI-NC does involve ion exchange mechanism that have been an influence on the nickel ions adsorption while varying the pH This observation is in line with the type I and II isotherm and positive $\triangle H^0$ value obtained, which indicates irreversible adsorption probably due to polar interactions.

3.4 Effect of other ions

The effect of other ions like Ca^{2+} and Cl^- on the adsorption process studied at different concentrations. The ions added to 50mg/L of nickel ions solutions and the contents were agitated for 60 min at 30^0C. The results had shown in the Fig. 4 reveals that low concentration of Cl^- does not affect the percentage of adsorption of nickel ions on ASI-NC, because the interaction of Cl^- at available sites of adsorbent through competitive adsorption is not so effective. While the concentration of other ion Ca^{2+} increases, the interference of these ions at available surface sites of the sorbent through competitive adsorption increases that, decreases the percentage adsorption. The interference was more in the presence of Ca^{2+} compared with Cl^- ion. This is so because ions with smaller hydrated radii decrease the swelling pressure within the sorbent and increase the affinity of the sorbent for such ions.

3.5 Adsorption Isotherms

Adsorption isotherm describes the relation between the amount or concentration of adsorbate that accumulates on the adsorbent and the equilibrium concentration of the dissolved adsorbate. Equilibrium studies were carried out by agitating a series of beakers containing 50 mL of nickel solutions of initial concentration 20 mg/L with 0.025 g of activated nano carbon at 30 ^{0}C with a constant agitation. Agitation was provided for 1.0 h, which is more than sufficient time to reach equilibrium.

3.5.1 Freundlich adsorption isotherm

The Freundlich adsorption isotherm is based on the equilibrium sorption on heterogeneous surfaces. This isotherm is derived from the assumption that the

adsorption sites are distributed exponentially with respect to heat of adsorption. The adsorption isotherm is expressed by the following equation

$$q_e = K_F C_e^{1/nF} \quad\text{..............(3)}$$

Which, can be linearized as

$$\ln q_e = \ln K_F + \frac{1}{n_F} \ln C_e \quad\text{.......................(4)}$$

Where, q_e is the amount of Nickel adsorbed at equilibrium (mg/g) and C_e is the concentration of nickel in the aqueous phase at equilibrium (ppm). K_F (L/g) and $1/n_F$ are the Freundlich constants related to adsorption capacity and sorption intensity, respectively.

The Freundlich constants K_F and $1/n_F$ were calculated from the slope and intercept of the $\ln q_e$ Vs $\ln C_e$ plot, and the model parameters are shown in Table 2. The magnitude of K_F showed that ASI-NC had a high capacity for nickel adsorption from the aqueous solutions studied. The Freundlich exponent, n_F, should have values in the range of 1 and 10 (i.e., $1/n_F < 1$) to be considered as favourable adsorption [5]. A $1/n_F$ value of less than 1 indicated that nickel is favorably adsorbed by ASI-NC. The Freundlich isotherm did not show a good fit to the experimental data as indicated by SSE and Chi-square statistics.

3.5.2 Langmuir adsorption isotherm

The Langmuir adsorption isotherm is based on the assumption that all sorption sites possess equal affinity to the adsorbate. The Langmuir isotherm [6] in a linear form can be represented as:

$$\frac{C_e}{q_e} = \frac{1}{q_m K_L} + \frac{C_e}{q_m} \quad\text{.............(5)}$$

Where q_e is the amount of nickel adsorbed at equilibrium (mg/g), C_e is the concentration of nickel in the aqueous phase at equilibrium (ppm), q_m is the maximum nickel uptake (mg/g), and K_L is the Langmuir constant related to adsorption capacity and the energy of adsorption (g/mg).

A linear plot of C_e/q_e Vs C_e was employed to determine the value of q_m and K_L the obtained data's were also presented in Table 2. The model predicted a maximum value that could not be reached in the experiments. The value of K_L decreased with an increase in the temperature. A high K_L value indicates a high adsorption affinity. Weber and Chakraborti expressed the Langmuir isotherm in term of dimensionless constant separation factor or equilibrium parameter (R_L) defined in the following equation:

$$R_L = \frac{1}{1 + K_L C_0} \quad\text{..................(6)}$$

Where, C_0 is the initial nickel concentration (ppm). Four scenarios can be distinguished:

The sorption isotherm is unfavorable when $R_L > 1$, the isotherm is linear when $R_L = 1$, the isotherm is favorable when $0 < R_L < 1$ and the isotherm is irreversible when $R_L = 0$. The values of dimensionless separation factor (R_L) for nickel removal were calculated at different concentrations and temperatures. As shown in Table 3, at all concentrations and temperatures tested the values of R_L for nickel adsorptions on the ASI-NC were less than 1 and greater than zero, indicating favorable adsorption.

The Langmuir isotherm showed a better fit to the adsorption data than the Freundlich isotherm. The fact that the Langmuir isotherm fits the experimental data well may be due to homogeneous distribution of active sites on the ASI-NC surface, since the Langmuir equation assumes that the adsorbent surface is energetically homogeneous.

3.5.3 Temkin adsorption isotherm:

The Temkin adsorption isotherm assumes that the heat of adsorption decreases linearly with the sorption coverage due to adsorbent-adsorbate interactions [7]. The Temkin isotherm equation is given as:

$$q_e = \frac{RT}{bT} \ln(K_T C_e) \quad\text{...............(7)}$$

Which, can be represented in the following linear form

$$q_e = \frac{RT}{b} \ln K_T + \frac{RT}{b} \ln C_e \quad\text{.................(8)}$$

Where, K_T (L/g) is the Temkin isotherm constant, b_T (J/mol) is a constant related to heat of sorption, R is the ideal gas constant (8.314 J/mol K), and T is absolute temperature (K). A plot of q_e versus $\ln C_e$ enables the determination of isotherm constants K_T and b_T from the slope and intercept, the model parameters are listed in Table 2. The Temkin isotherm appears to provide a good fit to the nickel adsorption data.

The adsorption energy in the Temkin model, b_T, is positive for Nickel adsorption from the aqueous solution, which indicates that the adsorption is endothermic. The experimental equilibrium curve is close to that predicted by Temkin model. Consequently, the adsorption isotherm of nickel on ASI-NC can be described reasonably well by the Temkin isotherm.

3.5.4 Hurkins-Jura adsorption isotherm

The Hurkins-Jura [8] adsorption isotherm can be expressed as

$$q_e = \sqrt{\frac{A_H}{B_H + \log C_e}} \quad\text{..................(9)}$$

This can rearranged as follows:

$$\frac{1}{q_e^2} = \frac{B_H}{A_H} - \frac{1}{A_H} \log C_e \quad\text{..............(10)}$$

Where, A_H (g^2/L) and B_H (mg^2/L) are two parameters characterizing the sorption equilibrium.

The isotherm equation accounts for multilayer adsorption and can be explained by the existence of a heterogeneous pore distribution. The Harkins–Jura isotherm parameters are obtained from the plots of of $1/q_e^2$ versus $\log C_e$

enables the determination of model parameters A_H and B_H from the slope and intercept.

3.5.5 Halsay adsorption isotherm

The Halsay [9] adsorption isotherm can be given as

$$q_e = exp\left(\frac{lnK_{Ha} - lnC_e}{n_{Ha}}\right) \dots\dots\dots(11)$$

A linear form of the isotherm can be expressed as follows

$$lnq_e = \frac{lnK_{Ha}}{n_{Ha}} - \frac{lnC_e}{n_{Ha}} \dots\dots\dots(12)$$

Where, K_{Ha} (mg/L) and n_{Ha} are the Halsay isotherm constants.

A plot of lnq_e Vs lnC_e, enables the determination of n_{Ha} and K_{Ha} from the slope and intercept. This equation is suitable for multilayer adsorption and the fitting of the experimental data to this equation attest to the heteroporous nature of adsorbent. The experimental data and the model predictions based on the non-linear form of the Halsay models. The model parameters are listed in Table 2. This result also shows that the adsorption of Nickel on ASI-NC was not based on significant multilayer adsorption. The Halsay model is also not suitable to describe the adsorption of nickel on ASI-NC, because this model also assumes a multilayer behavior for the adsorption of adsorbate onto adsorbent.

3.5.6 Redlich-Peterson adsorption isotherm

The Radlich-Peterson [10] adsorption isotherm contains three parameters and incorporates the features of Langmuir and Freundlich isotherms into a single equation. The general isotherm equation can be described as follows:

$$q_e = \frac{K_R C_e}{1 + a_R C_e^g} \dots\dots\dots(13)$$

The linear form of the isotherm can be expressed as follows:

$$ln\frac{C_e}{q_e} = glnC_e - lnK_R \dots\dots\dots(14)$$

Where, K_R (L/g) and a_R (L/mg) are the Radlich-Peterson isotherm constants and g is the exponent between 0 and 1. There are two limiting cases: Langmuir form for g = 1 and Henry's law for g = 0.

A plot of $ln\, C_e/q_e$ versus $ln\, C_e$ enables the determination of isotherm constants g and K_R from the slope and intercept. The values of K_R, presented in Table 2, indicate that the adsorption capacity of the ASI-NC decreased with an increase temperature. Furthermore, the value of g lies between 0 and 1, indicating favorable adsorption.

3.5.7 Dubinin-Radushkevich adsorption isotherm

The Dubinin-Radushkevich [11] adsorption isotherm is another isotherm equation. It is assumed that the characteristic of the sorption curve is related to the porosity of the adsorbent. The linear form of the isotherm can be expressed as follows:

$$lnq_e = lnQ_D - B_D\left[RTln\left(1 + \frac{1}{C_e}\right)\right]^2 \dots\dots\dots(15)$$

Where, Q_D is the maximum sorption capacity (mol/g), and B_D is the Dubinin-Radushkevich constant (mol^2/kJ^2). A plot of lnq_e Vs $R_T ln(1+1/C_e)$ enables the determination of isotherm constants B_D and Q_D from the slope and intercept.

3.5.8 Jovanovic adsorption isotherm

The model of an adsorption surface considered by Jovanovic[16] is essentially the same as that considered by Langmuir. The Jovanovic model leads to the following relationship [12]:

$$q_e = q_{max}\left(1 - e^{K_J C_e}\right) \dots\dots\dots(16)$$

The linear form of the isotherm can be expressed as follows:

$$lnq_e = lnq_{max} - K_J C_e \dots\dots\dots(17)$$

Where, K_J (L/g) is a parameter. q_{max} (mg/g) is the maximum Nickel (II) uptake.

The q_{max} is obtained from a plot of $ln\, q_e$ and C_e. Their related parameters are listed in Table 2. By comparing the values of the error functions, it was found the Langmuir and Temkin models are best to fit the Nickel adsorption on the ASI-C. Both models show a high degree of correlation. This is clearly confirming the good fit of Langmuir and Temkin models with the experimental data for removal of nickel from the solution.

3.5.9 The Brunauer-Emmett-Teller (BET) isotherm model

Brunauer-Emmett-Teller (BET) isotherm is a theoretical equation, most widely applied in the gas-solid equilibrium systems [13]. It was developed to derive multilayer adsorption systems with relative concentration ranges from 10 to 50 mg/L corresponding to a monolayer coverage lying between 10 and 30 mg/L. Its extinction model related to liquid-solid interface is exhibited as:

$$q_e = \frac{q_S C_{BET} C_e}{(C_S - C_e)[1 + (C_{BET} - 1)(C_e/C_S)]} \dots\dots\dots(18)$$

Where, C_{BET}, C_s, q_s and q_e are the BET adsorption isotherm (L/mg), adsorbate monolayer saturation concentration (mg/L), theoretical isotherm saturation capacity (mg/g) and equilibrium adsorption capacity (mg/g), respectively. As C_{BET} and C_{BET} (C_e/C_s) is much greater than 1,

In the linear form as used is represented as

$$\frac{C_e}{q(C_S - C_e)} = \frac{1}{q_S C_{BET}} + \left(\frac{C_{BET} - 1}{q_S C_{BET}}\right)\left(\frac{C_e}{C_S}\right) \dots\dots\dots(19)$$

Where, C_e is equilibrium Concentration (mg/l), C_s is adsorbate monolayer saturation concentration (mg/l) and C_{BET} is BET adsorption relating to the energy of surface interaction (l/mg).

3.6 Kinetic parameters

The rate and mechanism of the adsorption process can be elucidated based on kinetic studies. Nickel adsorption on solid surface may be explained by two distinct mechanisms: (1) An initial rapid binding of nickel molecules on the adsorbent surface; (2) relatively slow intra-particle diffusion. To analyze the adsorption kinetics of the nickel, the pseudo-first-order, the pseudo-second-order, and intra-particle diffusion models were applied [14]. Each of these models and their linear modes of them equations presented in below.

Kinetic Models and Their Linear Forms

Model	Nonlinear Form	Linear Form	Number of Equation
Pseudo-first-order	$dq_t/d_t = k_1(q_e-q_t)$	$\ln(q_e-q_t) = \ln q_e - k_1 t$	(20)
Pseudo-second-order	$dq_t/d_t = k_2(q_e-q_t)^2$	$t/q_t = 1/k_2 q_e^2 + (1/q_e)t$	(21)

Where, q_e and q_t refer to the amount of nickel adsorbed (mg/g) at equilibrium and at any time, t (min), respectively and k_1 (1/min), k_2 (g/mg min) are the equilibrium rate constants of pseudo-first order and pseudo-second order models, respectively.

Pseudo-first order model is a simple kinetic model, which was proposed by Lagergren during 1898 and is used for estimation of the surface adsorption reaction rate. The values of $\ln(q_e - q_t)$ were linearly correlated with t. The plot of $\ln(q_e - q_t)$ Vs t should give a linear relationship from which the values of k_1 were determined from the slope of the plot. In many cases, the first-order equation of Lagergren does not fit well with the entire range of contact time and is generally applicable over the initial stage of the adsorption processes.

In the pseudo-second order model, the slope and intercept of the t/q_t Vs t plot were used to calculate the second-order rate constant, k_2. The values of equilibrium rate constant (k_2) are presented in Table 5. According to Table 5, the value of R^2 (0.999) related to the pseudo-second order model revealed that nickel adsorption followed this model.

Nevertheless, pseudo-first order and pseudo-second order kinetic models cannot identify the mechanism of diffusion of nickel into the adsorbent pores.

3.6.1 Simple Elovich Model:

The simple Elovich model [15] is expressed in the form,

$$q_t = \alpha + \beta \ln t \quad \ldots\ldots\ldots\ldots\ldots(22)$$

Where, q_t is the amount adsorbed at time t, α and β are the constants obtained from the experiment. A plot of q_t Vs ln 't' should give a linear relationship for the applicability of the simple Elovich kinetic. The Elovich kinetics of nickel on to ASI-NC for various initial concentrations (10, 20, 30, 40 and 50 mg/L) of volume 50 mL (each), adsorbent dose 0.025g, temperature 30 ºC and pH 6.5.

3.6.2 The Elovich equation

The Elovich model equation is generally expressed as

$$dq_t/d_t = \alpha \exp(-\beta q_t) \quad \ldots\ldots\ldots\ldots(23)$$

Where; α is the initial adsorption rate (mg g^{-1} min^{-1}) and β is the desorption constant (g/mg) during any one experiment. To simplify the Elovich equation [16] assumed $\alpha\beta t \gg t$ and by applying boundary conditions $q_t = 0$ at t= 0 and $q_t = q_t$ at t = t Eq.(23) becomes:

$$q_t = 1/\beta \ln(\alpha\beta) + 1/\beta \ln t \quad \ldots\ldots\ldots (24)$$

If nickel ions adsorption fits with the Elovich model, a plot of q_t vs. ln(t) should yield a linear relationship with a slope of $(1/\beta)$ and an intercept of $(1/\beta)\ln(\alpha\beta)$. The Elovich model parameters α, β, and correlation coefficient (γ) are summarized in table 5. The experimental data such as the initial adsorption rate (α) adsorption constant (β) and the correlation co-efficient (γ) calculated from this model indicates that the initial adsorption (α) increases with temperature similar to that of initial adsorption rate (h) in pseudo-second–order kinetics models. This may be due to increase the pore or active site on the ASI-NC adsorbent.

3.6.3 The Intraparticle diffusion model

The kinetic results were analyzed by the Intraparticle diffusion model [17, 20] to elucidate the diffusion mechanism. The model is expressed as:

$$q_t = K_{id} t^{1/2} + I \quad \ldots\ldots\ldots\ldots\ldots (25)$$

Where, 'I' is the intercept and K_{id} is the intra-particle diffusion rate constant. The intercept of the plot reflects the boundary layer effect. Larger the intercept, greater is the contribution of the surface sorption in the rate controlling step. The calculated diffusion coefficient K_{id} values are listed in Table 6. The K_{id} value was higher at the higher concentrations. Intraparticle diffusion is the sole rate-limiting step if the regression of q_t versus $t^{1/2}$ is linear and passes through the origin. In fact, the linear plots at each concentration did not pass through the origin. This deviation from the origin is due to the difference in the rate of mass transfer in the initial and final stages of the sorption. This indicated the existence of some boundary layer effect and further showed that Intraparticle diffusion was not the only rate-limiting step.

It is clear from the Table 5 that the pseudo- second-order kinetic model showed excellent linearity with high correlation coefficient ($R^2 > 0.99$) at all the studied concentrations in comparison to the other kinetic models.

In addition the calculated q_e values also agree with the experimental data in the case of pseudo-second-order kinetic model. It is also evident from Table 5 that the values of the rate constant k_2 decrease with increasing initial nickel concentrations. This is due to the lower competition for the surface active sites at lower concentration but at higher concentration the competition for the surface active sites will be high and consequently lower sorption rates are obtained.

3.7. Thermodynamic treatment of the adsorption process

Thermodynamic parameters associated with the adsorption, via standard free energy change (ΔG^0), standard enthalpy change (ΔH^0), and standard entropy change (ΔS^0) were calculated as follows. The free energy of adsorption process considering the adsorption equilibrium constant K_0 is given by the equation

$$\Delta G^0 = -RT \ln K_0 \quad \dots\dots\dots\dots\dots\dots\dots (26)$$

Where, ΔG^0 is the free energy of adsorption (kJ/mol), T is the temperature in Kelvin and R is the universal gas constant(8.314 J mol/K).The adsorption distribution coefficient K_0 for the sorption reaction was determined from the slope of the plot of $\ln(q_e/C_e)$ against C_e at different temperature. The adsorption distribution coefficient may be expressed in terms of enthalpy change (ΔH^0) and entropy change (ΔS^0) as a function of temperature,

$$\ln K_0 = (\Delta H^0/RT)+(\Delta S^0/R) \quad \dots\dots\dots\dots.(27)$$

Where, ΔH^0 is the standard heat change of sorption (kJ/mol) and ΔS^0 is standard entropy change (kJ/mol). The value of ΔH^0 and ΔS^0 can be obtained from the slope and intercept of plot of $\ln K_0$ against $1/T$. The value of thermodynamic parameter calculated from equation 26 and 10 are shown in table 4. The thermodynamic treatment of the sorption data indicates that ΔG^0 values were negative at all temperature. The results point out that physisorption is much more favorable for the adsorption of nickel ions. The positive values of ΔH^0 show the endothermic nature of adsorption and it governs the possibility of physical adsorption [18]. Because in the case of physical adsorption, while increasing the temperature of the system, the extent of nickel ions adsorption increases, this rules out the possibility of chemisorptions. The low ΔH^0 value depicts nickel ions is physisorbed onto adsorbent ASI-NC.

The negative ΔG^0 values table 4 were conform the spontaneous nature of adsorption nickel ions onto ASI-NC**.** The lesser values of ΔG^0 suggest that adsorption is physical adsorption process. The positive values of ΔS^0 in table 4, showed increased randomness of the solid solution interface during the adsorption of nickel ion onto ASI-NC.

In order to support that physical adsorption is the predominant mechanism, the values of activation energy (E_a) and sticking probability (S^*) were calculated from the experimental data. They were calculated using modified Arrhenius type equation related to surface coverage (θ) as follows:

$$\theta = \left(1 - \frac{C_e}{C_i}\right) \quad \dots\dots\dots\dots. (28)$$

$$S^* = (1-\theta)_e \frac{-E_a}{RT} \quad \dots\dots\dots (29)$$

The sticking probability, S^*, is a function of the adsorbate/adsorbent system under consideration but must satisfy the condition $0 < S^* < 1$ and is dependent on the temperature of the system. The values of Ea and S^* can be calculated from slope and intercept of the plot of $\ln(1-\theta)$ versus $1/T$ respectively and are listed in Table 4.

From Table 4 it is clear that the reaction is spontaneous in nature as ΔG^0 values are negative at all the temperature studied. Again positive ΔH^0 value confirms that the sorption is endothermic in nature. The positive value of ΔS^0 reflects the affinities of the adsorbents for the nickel. The result as shown in Table 4 indicate that the probability of the nickel to stick on surface of biomass is very high as $S^* << 1$, these values confirm that, the sorption process is physisorption.

3.8 Desorption studies

Desorption studies help to elucidate the nature of adsorption and recycling of the spent adsorbent and the nickel ions. If the adsorbed nickel ions can be desorbed using neutral pH water, then the attachment of the nickel ions of the adsorbent is by weak bonds. The effect of various reagents used for desorption studies. The results indicate that hydrochloric acid is a better reagent for desorption, because we could get more than 90% removal of adsorbed nickel ions. The reversibility of adsorbed nickel ions in mineral acid or base is in agreement with the pH dependent results obtained. The desorption of nickel ions by mineral acids and alkaline medium indicates that the nickel ions was adsorbed onto the ASI-NC through physisorption as well as by chemisorptions mechanisms [19].

IV. CONCLUSION

ASI-NC prepared from Syringodium Isoetifolium Leaves was found effective in removing nickel ion from aqueous solution. The adsorption is faster and the rate is mainly controlled by intra-particle diffusion. Using the sorption equation obtained from the Langmuir and Freundlich isotherms, it was found that ASI-NC is an effective one for the removal of nickel ion. The equilibrium data conformed well to the Langmuir and BET isotherm models. The temperature variation study showed that the

nickel ion adsorption is endothermic and spontaneous with increased randomness at the solid solution interface. Significant effect on adsorption was observed on varying the pH of the nickel ion solution. pH dependent results and desorption of metal ion in mineral acid suggest that the adsorption of nickel ions on ASI-NC involves chemisorptions as well as physisorption mechanism.

ACKNOWLEDGEMENT

REFERENCES

[1] Zolfaghari, G., Esmaili-Sari, A., Anbia, M., Younesi, H. and Ghasemian, M.B. "A zinc oxide-coated nanoporous carbon adsorbent for lead removal from water" Optimization, equilibrium modeling, and kinetics studies, (2013). *International Journal of Environmental Science and Technology*, 10 (2), 325-340.

[2] Memarian, R. and Ramamurthy, A.S., "Modeling of lead and cadmium uptake by plants in the presence of surfactants" (2013), *Environmental Monitoring and Assessment*, 185 (3), 2067-2071.

[3] Vijayaraghavan, K. and Joshi, U.M. Chicken Eggshells "Remove Pb(II) Ions from Synthetic Wastewater" (2013), *Environmental Engineering Science*, 30 (2), 67-73.

[4] Shukla, N.B. and Madras, G. "Kinetics of adsorption of methylene blue and rhodamine 6G on acrylic acid-based superabsorbents" (2012), *Journal of Applied Polymer Science*, 126 (2), 463-472.

[5] Usman, A.R.A., Sallam, A.S., Al-Omran, A., El-Naggar, A.H., Alenazi, K.K.H., Nadeem, M. and Al-Wabel, M.I. "Chemically Modified Biochar Produced from Conocarpus Wastes: An Efficient Sorbent for Fe(II) Removal from Acidic Aqueous Solutions" (2013), *Adsorption Science & Technology*, 31 (7), 625-640.

[6] Diaz, P.V., Medina, E.C., Nunez, F.U. and Fabila, M.G. "Reuse of Citrullus Lanatus Peel As Biosorbent to Remove Aluminum in Aqueous Phase" (2013), *Fresenius Environmental Bulletin*, 22 (5), 1432-1440.

[7] Bulgariu, L., Lupea, M., Bulgariu, D., Rusu, C. and Macoveanu, M. "Equilibrium Study of Pb(Ii) and Cd(Ii) Biosorption from Aqueous Solution on Marine Green Algae Biomass" (2013), *Environmental Engineering and Management Journal*, 12 (1), 183-190.

[8] Duran-Blanco, J.M., Lopez-Munoz, B.E. and Olguin, M.T. "Influence of pH on U(VI) Adsorption using a Thermally-Treated Mg-Al Hydrotalcite and a Natural Zeolite in a Batch System" (2013), *Separation Science and Technology*, 48 (5), 797-804.

[9] Vistuba, J.P., Nagel-Hassemer, M.E., Lapolli, F.R. and Recio, M.A.L. "Simultaneous adsorption of iron and manganese from aqueous solutions employing an adsorbent coal" (2013), *Environmental Technology*, 34 (2), 275-282.

[10] Frendlich H. "The dye adsorption is losungen (Adsorption in Solution)" (1906), *Z Phys. Chem.*,57, 385 – 470.

[11] Taghdiri, M. and Zamani, N. "Hexamine adsorption study on activated carbon from aqueous solutions for application in treatment of hexamine industrial wastewater" (2013), *International Journal of Environmental Science and Technology*, 10 (1), 19-26.

[12] Bulgariu, L., Hlihor, R.M., Bulgariu, D. and Gavrilescu, M. "Sorptive Removal of Cadmium(II) Ions from Aqueous Solution by Mustard Biomass" (2012), *Environmental Engineering and Management Journal*, 11 (11), 1969-1976.

[13] Hadi, M., Mckay, G., Samarghandi, M.R., Maleki, A. and Aminabad, M.S. "Prediction of optimum adsorption isotherm: comparison of chi-square and Log-likelihood statistics" (2012), *Desalination and Water Treatment*, 49 (1-3), 81-94.

[14] Langmuir I. "The adsorption of gases plane surfaces of glass, mica and platinum" (1918), *J. Am. Soc.*, 579, 1361 – 1403.

[15] Hang, X.F., Xu, Y.M., Wang, L., Sun, Y.B., Lin, D.S., Sun, Y., Qin, X. and Wan, Q. "Sorption of Pb^{2+} on mercapto functionalized sepiolite" (2013), *Chemosphere*, 90 (2), 548-555.

[16] Zhou, Y.N., Wang, Z., Zhang, Q., Xi, X.J., Zhang, J. and Yang, W.T. "Equilibrium and thermodynamic studies on adsorption of BSA using PVDF microfiltration membrane" (2012), *Desalination*, 307, 61-67.

[17] Khan, A A, Singh, R P. "Adsorption thermodynamics of carbofuran on Sn (IV) arsenosilicate in H^+, Na^+ and Ca^{2+} forms" (1987), *Colloid & Surfaces* (24) 33 – 42.

[18] Ghosh, A. and Das Saha, P. "Optimization of Nickel adsorption by chemically modified fly ash using response surface methodology modeling" (2012), *Desalination and Water Treatment*, 49 (1-3), 218-226.

[19] Chien S H. and Clayton.W R. "Application of Elovich Equation to the kinetics of Phosphate release and sorption on soil" (1980), *Soil Sci. Sco. Am, J.*, 44, 265 – 268.

[20] W. J. Weber and Morris J C. "Kinetics of adsorption on Carbon from solution" (1964), *J. Sanitary Engg. Div*. 90, 79.

Table: 1: Equilibrium Parameters for the adsorption of nickel (II) ion onto ASI-NC

M_0	Ce (mg / L)				Qe (mg / g)				Removed (%)			
	30 °C	40 °C	50 °C	60 °C	30 °C	40 °C	50 °C	60 °C	30 °C	40 °C	50 °C	60 °C
10	2.451	1.951	1.701	1.676	15.10	16.10	16.60	16.65	75.49	80.49	82.99	83.24
20	3.951	3.702	3.461	2.951	32.10	32.60	33.08	34.10	80.25	81.49	82.69	85.24
30	7.221	6.652	5.951	5.602	45.56	46.70	48.10	48.80	75.93	77.83	80.16	81.33
40	9.972	9.222	8.809	8.338	60.06	61.56	62.38	63.32	75.07	76.95	77.98	79.16
50	14.20	13.75	13.47	12.74	71.60	72.50	73.05	74.51	71.60	72.50	73.05	74.51

Table: 2: Langmuir and Freundlich Isotherm Parameter for the adsorption of nickel (II) ion onto ASI-NC

Model	Constant	Temperature (°C)			
		30	40	50	60
Freundlich	K_f (mg/g) $(L/mg)^{1/n}$	8.241	10.62	12.39	13.32
	n	1.176	1.301	1.384	1.391
Langmuir	Q_m (mg/g)	228.0	161.8	140.0	141.2
	b (L/mg)	0.034	0.062	0.085	0.093
Temkin	b_T (J/mol)	31.44	29.06	27.81	28.34
	K_T (L/mg)	0.851	0.948	1.003	1.023
Hurkins-Jura	A_H (g^2/L)	-204.8	-245.2	-273.4	-285.4
	B_H (mg^2/L)	-1.058	-1.037	-1.020	-0.997
Halsay	K_{Ha} (mg/L)	11.94	21.62	32.53	36.68
	n_{Ha}	1.176	1.301	1.384	1.391
Radlich-Peterson	g	0.150	0.231	0.277	0.281
	K_R (L/g)	0.121	0.094	0.081	0.075
Dubinin-Radushkevich	q_s (mg/g)	65.80	62.94	62.72	66.45
	$K_D \times 10^{-4}$ mol^2 kJ^{-2}	1.506	1.491	1.486	1.496
Jovanovic	K_J (L/g)	0.119	0.117	0.115	0.119
	q_{max} (mg/g)	16.07	17.74	19.21	19.88
BET	C_{BET} (L/mg)	6.265	3.754	4.897	6.194
	qs (mg/g)	0.160	0.266	0.204	0.161

Table: 3: Dimensionless Separation factor (R_L) for the adsorption of nickel (II) ion onto ASI-NC

(C_i)	Temperature °C			
	30°C	40°C	50°C	60°C
10	0.540	0.392	0.319	0.302
20	0.369	0.244	0.190	0.178
30	0.281	0.177	0.135	0.126
40	0.227	0.139	0.105	0.098
50	0.190	0.114	0.086	0.080

Table: 4: Thermodynamic Parameter for the adsorption of nickel (II) ion onto ASI-NC

C_0	ΔG°				ΔH°	ΔS°	E_a	S^*
	30° C	40° C	50° C	60° C				
10	-2834.3	-3688.6	-4255.7	-4437.9	13.57	54.62	1019.8	0.0032
20	-3531.3	-3857.2	-4200.3	-4855.6	9.484	42.75	7849.6	0.0089
30	-2894.0	-3267.6	-3750.5	-4073.8	9.313	40.28	7332.0	0.0131
40	-2777.1	-3136.4	-3395.3	-3694.3	6.347	30.18	4897.7	0.0355
50	-2329.3	-2522.7	-2678.4	-2970.0	3.944	20.66	2880.5	0.0909

Table: 5: The Kinetic Parameters for the adsorption of nickel (II) ion onto ASI-NC

| C₀	Temp °C	Pseudo Second Order				Elovich Model			Intraparticle Diffusion		
		q_e	k_2	γ	h	α	β	γ	K_{id}	γ	C
10	**30**	15.31	0.016	0.978	3.716	2.979	3.562	9.971	1.801	9.877	1.866
	40	17.42	0.010	0.978	2.906	6.795	4.787	9.898	1.445	9.869	1.642
	50	17.38	0.016	0.984	4.946	3.016	7.172	9.900	8.986	9.896	1.755
	60	17.38	0.017	0.981	5.278	5.642	7.557	9.911	8.469	9.907	1.765
20	**30**	35.49	0.003	0.984	4.283	4.178	2.003	9.954	1.784	9.929	1.571
	40	35.74	0.004	0.979	4.845	6.173	2.097	9.909	1.66	9.896	1.605
	50	36.09	0.004	0.982	5.639	9.854	2.200	9.904	1.535	9.922	1.639
	60	36.58	0.005	0.979	6.536	2.285	2.427	9.921	1.339	9.939	1.684
30	**30**	48.59	0.004	0.979	8.731	5.699	1.997	9.958	1.210	9.880	1.656
	40	50.32	0.004	0.985	10.21	4.710	1.837	9.899	1.268	9.871	1.665
	50	52.34	0.003	0.984	9.347	2.043	1.576	9.922	1.454	9.863	1.645
	60	51.95	0.005	0.985	13.38	8.262	1.856	9.900	1.197	9.865	1.702
40	**30**	64.52	0.004	0.983	15.27	4.878	1.362	9.938	1.332	9.884	1.646
	40	66.02	0.003	0.978	15.00	4.938	1.336	9.915	1.331	9.892	1.654
	50	66.66	0.004	0.981	16.36	6.765	1.369	9.962	1.276	9.913	1.670
	60	67.62	0.004	0.985	16.85	7.741	1.370	9.918	1.254	9.924	1.681
50	**30**	76.55	0.002	0.979	12.63	4.483	1.162	9.920	1.340	9.911	1.602
	40	77.59	0.002	0.985	12.75	4.466	1.145	9.913	1.343	9.932	1.607
	50	77.76	0.002	0.979	13.77	7.295	1.212	9.920	1.250	9.880	1.628
	60	79.51	0.002	0.981	13.20	5.096	1.133	9.949	1.320	9.880	1.622
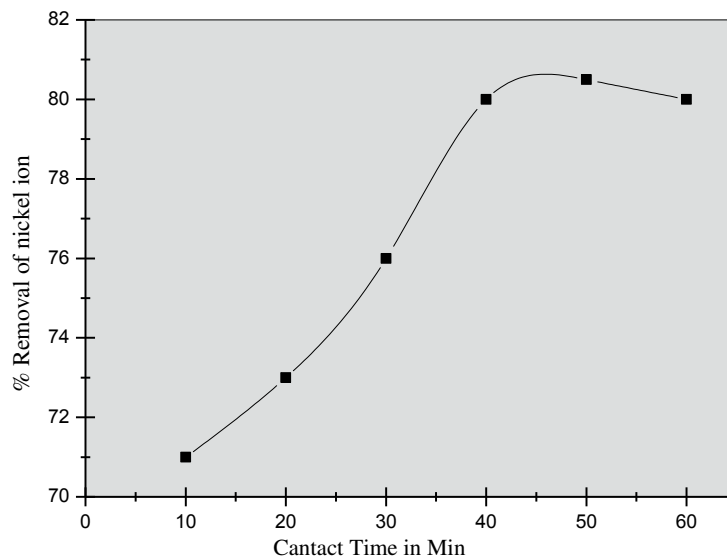
Fig:1- Effect of contact time on the removal of nickel ion

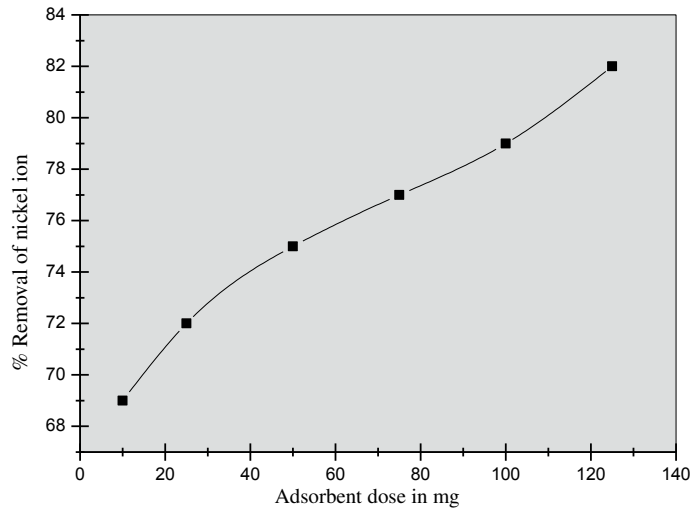[Ni]=20 mg/L;Temprature 30°C;Adsorbent dose=25mg/50ml

Fig; 2- Effect of Adsorbent dose on the removal of nickel ion
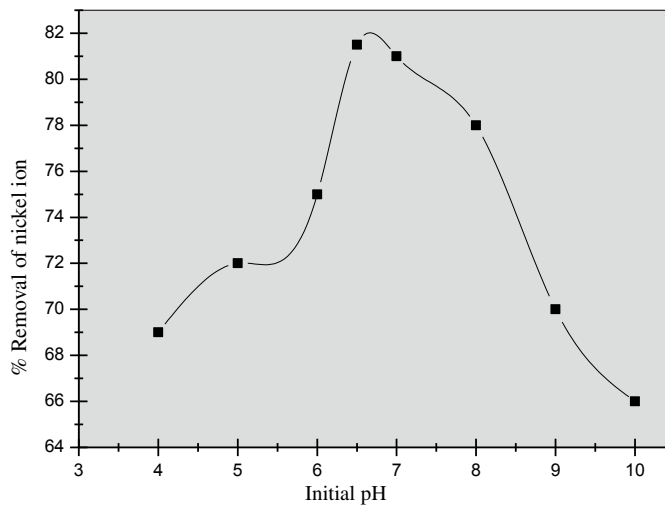[Ni]= 20mg/L; Contact time =60 min; Temprature 30^0C

Fig;3- Effect of initial pH on the removal of nickel ion
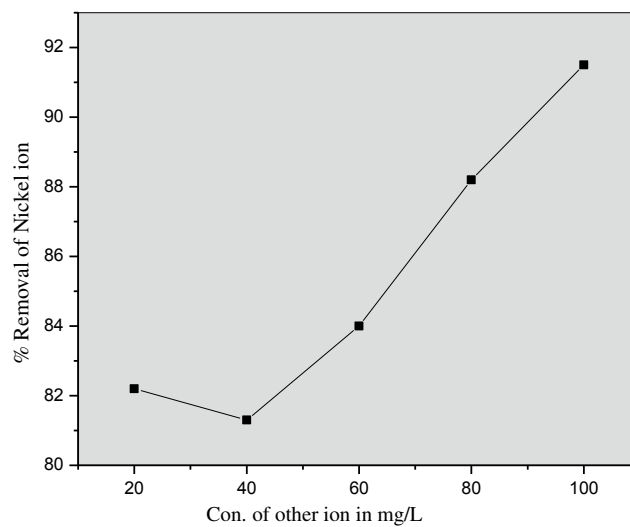[Ni]= 20 mg/L;Temprature 30^oC; Adsorbent dose=25mg/50ml

Fig.4-Effect of ionic strength on the adsorption of nickel ion
[Ni]= 20 mg/L;pH=6.5; Adsorbent dose=25mg/50 ml